

## Large Thermoelectric Effects in Unconventional Superconductors

T. Lofwander<sup>1,\*</sup> and M. Fogelstrom<sup>2,y</sup><sup>1</sup>Department of Physics & Astronomy, Northwestern University, Evanston, IL 60208<sup>2</sup>Applied Quantum Physics, MC2, Chalmers, S-41296 Goteborg, Sweden

(dated: December 23, 2021)

We present analytic and numerical results for the thermoelectric effect in unconventional superconductors with a dilute random distribution of impurities, each scattering isotropically but with a phase shift intermediate between the Born and unitary limits. The thermoelectric response function has a linear temperature dependence at low temperatures, with a slope that depends on the impurity concentration and phase shift. Although the thermoelectric effect vanishes identically in the strict Born and unitary limits, even a small deviation of the phase shift from these limits leads to a large response, especially in clean systems. We also discuss possibilities of measuring counter-flowing supercurrents in a SQUID-setup. The non-quantized thermoelectrically induced flux can easily be of the order of a percent of the flux quantum in clean systems at <sup>4</sup>He temperatures.

PACS numbers: 74.25.Fy, 74.72.-h

## I. INTRODUCTION

Electronic charge and heat transport measurements can give important information about the microscopic properties of high- $T_c$  and other unconventional superconductors.<sup>1,2,3,4,5,6,7,8,9,10,11,12,13,14,15,16,17,18,19,20</sup> Of particular interest is the low-temperature regime, where electronic properties are believed to be controlled by elastic impurity scattering. This is the case, because in an unconventional superconductor with an order parameter changing sign at some points on the Fermi surface (for example the d-wave order parameter), elastic scattering by even a small concentration of impurities leads to pair breaking, and the formation of an impurity band of width around the Fermi level. These low-lying excitations, are responsible for a universal limit at low temperatures  $T \rightarrow 0$ , where the charge and heat conductances become independent of the scattering properties of the impurities. This low-energy behavior was first predicted by Lee<sup>16</sup> for the zero-frequency charge conductance, and was later extended to include the heat conductance by Graf et al.<sup>18</sup>

The universal character of the  $T \rightarrow 0$  heat conductance was seen experimentally in Refs. [2,4,6,8,10,11]. A series of recent related experiments on the temperature dependence of the heat conductance approaching the universal limit,<sup>12</sup> microwave conductivity,<sup>13</sup> and STM spectroscopy of quasiparticle impurity states,<sup>21</sup> have all indicated that impurity scattering in the cuprates might not be in the strict unitary or Born limits. Limiting the discussion to isotropic scattering, this means that the impurity potential  $u_0$  is of intermediate size, and the corresponding s-wave scattering phase shift  $\phi_0 = \arctan(N_F u_0)$  has some intermediate value  $0 < \phi_0 < \pi/2$ . Here is  $N_F$  the density of states at the Fermi level in the normal state. If this is the case, electron-hole symmetry is explicitly broken near each impurity and the global electron-hole symmetry is broken for a homogeneous dilute distribution of such impurities.<sup>22,23,24,25</sup> This has direct consequences for the heat and charge transport

coefficients,<sup>18</sup> but leads also to large thermoelectric effects. A fact that was previously noted in connection to the heavy fermion systems by Ar et al.<sup>23,24</sup> In the present paper we report an extensive analysis of electron-hole symmetry breaking by elastic impurity scattering, and its effect on the transport coefficients in unconventional superconductors, with an emphasis on the d-wave cuprates at low temperatures.

Previous work on thermoelectric effects in the heavy fermion superconductors<sup>23,24,26</sup> were limited to situations in which the energy-dependent broadening of the quasiparticle states can be neglected, i.e. when the imaginary part of the impurity self-energy satisfies  $\text{Im} \Sigma \ll \text{Re} \Sigma$ . This approximation is expected to be good at high temperatures,  $T < T_c$ , but fails at lower temperatures. In fact, in the temperature regime  $T \sim T_c$  of high current interest, where effects of universality become of importance, the impurity renormalization is the dominant energy scale and the problem has to be considered anew.

Our results can be summarized as follows. (1) For intermediate phase shifts, the thermoelectric response function  $\mathcal{S}(T)$  is in general large, which leads to counter-flowing supercurrents detectable e.g. as a thermally induced magnetic flux in a ring setup.<sup>27,28,29,30,31</sup> (2) At low temperatures  $T \rightarrow 0$ ,  $\mathcal{S}(T)$  scales linearly with temperature, with a non-universal slope that grows large in clean systems.

## II. ELECTRON-HOLE SYMMETRY BREAKING AND GIANT THERMOELECTRIC EFFECTS

To compute the response to a thermal gradient  $\nabla T$  and an electric field  $E(\mathbf{r})$ , we need to evaluate the charge current  $\mathcal{J}_e$  as well as the heat current  $\mathcal{J}_h$ . In the linear response, the observable response functions such as the heat and charge conductivities, can conveniently be expressed in terms of response functions  $L_{\alpha\beta}$  that are

defined as

$$\hat{\mathcal{L}} = \begin{pmatrix} L_{11} & L_{12} \\ L_{21} & L_{22} \end{pmatrix} \cdot \frac{1}{T} : \quad (1)$$

This particular choice of forces ensures that the Onsager relations  $L_{12} = L_{21}$  are fulfilled (see e.g. Ref. [32]).

Contrary to the two diagonal terms  $L_{11}$  and  $L_{22}$  in Eq. (1), the thermoelectric coefficients  $L_{12} = L_{21}$  require an electron-hole asymmetry around the Fermi energy in order to be non-zero. In the normal state, to quasiclassical accuracy, i.e. to leading order in small parameters  $s = v_F T = T/T_F, 1 = p_F v_F, \dots$ , there is no such electron-hole asymmetry in the theory and the thermoelectric coefficients vanish,  $L_{12}^N = L_{21}^N = 0$ . Here  $v_F = v_F = T_c$  the superconducting coherence length, and  $T_F, p_F$ , and  $v_F$  are the Fermi temperature, momentum and velocity, respectively. This result holds also in the superconducting phase when the order parameter has the conventional s-wave symmetry.<sup>28</sup> However, for unconventional superconductors this is not the case: impurity scattering is pair-breaking and potential scattering on an impurity site induces a non-vanishing electron-hole asymmetry already to leading order in the small parameters [22,23,24,25]. To illustrate this, we consider a superconductor having an order parameter with a vanishing Fermi surface average,  $\langle p_F \rangle = 0$ , in which case the equilibrium-state impurity  $\hat{\mathcal{L}}_{\text{imp}}$  matrix in Nambu (electron-hole) space has the form

$$\hat{\mathcal{L}}_{\text{imp}}^R(\epsilon) = \frac{\sin \delta_0 \cos \delta_0 \hat{1} + \sin \delta_0 \frac{R}{R} \langle p_F \rangle g_3^R(\epsilon; \delta_0)}{N_F \cos^2 \delta_0 \sin^2 \delta_0 \left[ \langle p_F \rangle g_3^R(\epsilon; \delta_0) \right]}; \quad (2)$$

where the diagonal component of the equilibrium quasiclassical Green's function is  $g_3^R = \frac{1}{\epsilon} = \frac{R}{R} \left[ \frac{R}{R} = \frac{1}{j(\epsilon_F)^2} (\epsilon^2) \right]$ . The electron-hole asymmetric scattering becomes explicit when we examine the electron (11) and hole (22) parts:

$$t_{11(22)}^R = \frac{1}{\cos \delta_0 \sin \delta_0 \frac{R}{R} \langle p_F \rangle g_3^R(\epsilon; \delta_0)}; \quad (3)$$

In particular, multiple scattering on the impurity leads to resonances at  $\epsilon = \epsilon_{\text{res}}(\delta_0)$  for electron-like excitations and at  $\epsilon = +\epsilon_{\text{res}}(\delta_0)$  for hole-like excitations. These impurity resonances become virtual bound states localized at the impurity in the strong scattering limit,  $\delta_0 \rightarrow \pi/2$  [33]. This also implicates that electrons and holes have different energy dependent scattering life times at intermediate phase shifts.<sup>22</sup>

We assume that the impurities are randomly distributed with an average small concentration  $n_i$ , that is absorbed in the normal state elastic scattering rate  $\tau_0^{-1} = 2 = 2n_i \sin^2 \delta_0 = N_F$ . Within the usual impurity averaging technique<sup>34</sup> the impurity self energy has the form

$$\hat{\mathcal{L}}_{\text{imp}}^R(\epsilon) = \frac{R}{0} \left( \hat{1} + \frac{R}{3} \right) \hat{3} = n_i \hat{\mathcal{L}}_{\text{imp}}^R(\epsilon); \quad (4)$$

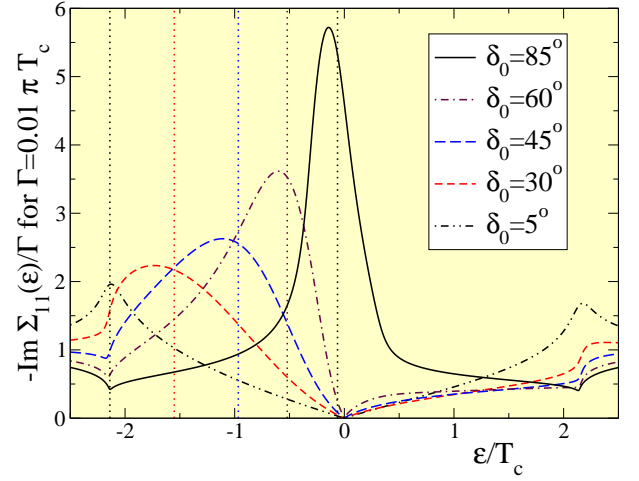


FIG. 1: The imaginary part of  $\hat{\mathcal{L}}_{11}^R$  shown for different normal state scattering phase shifts  $\delta_0$  for a d-wave superconductor with  $\langle p_F \rangle = \delta_0 \cos(2 p_F)$ . There is a substantial asymmetry in  $\hat{\mathcal{L}}_{11}^R(\epsilon)$  around  $\epsilon = 0$ . The dashed vertical lines indicate the single-impurity resonance energies  $\epsilon_{\text{res}}(\delta_0)$  for an electron-like quasiparticle at the corresponding phase shifts. The resonance energy of the single impurity self energy is carried over to the self-consistently computed self energy describing the randomly distributed impurities, but slightly shifted away from the Fermi level:  $\epsilon_{\text{res}}(\delta_0)$ . The hole component,  $\hat{\mathcal{L}}_{22}^R$ , is related to the electron component as  $\hat{\mathcal{L}}_{22}^R(\epsilon) = \frac{R}{0} \frac{R}{3} = \left[ \frac{R}{11}(\epsilon) \right]$ .

The term proportional to the third Pauli matrix in electron-hole space,  $\hat{3}$ , gives the impurity renormalization of the energy,  $\tilde{\epsilon}^R = \frac{R}{3}$ . The unit term,  $\frac{R}{0}(\epsilon)$ , drops out of the equations for the equilibrium state, but in fact enters the transport equations describing the non-equilibrium state.  $\frac{R}{0}(\epsilon)$  explicitly breaks electron-hole symmetry, which leads to the thermoelectric effect we study below. In general we can not expect the unit term to either vanish or to be small, although it vanishes in the strict Born and unitary limits. The induced asymmetry is shown for the electron part  $\hat{\mathcal{L}}_{11}^R = \frac{R}{0} + \frac{R}{3}$  in Fig. 1.

The response functions  $\hat{\mathcal{L}}$ , calculated to lowest order in the small parameters  $s$ , are conveniently computed through the quasiclassical Keldysh propagator  $\hat{\mathcal{G}}^K$ , evaluated to linear order in the forces. Amazingly,  $\hat{\mathcal{G}}^K$  has a closed form in which the self-consistently computed equilibrium Green's function  $\hat{\mathcal{G}}_0^R$ , order parameter  $\hat{\Delta}^R$ , and impurity self-energies  $\hat{\mathcal{L}}_{\text{imp}}^R$  serve as input.<sup>18,35</sup> A complication is that  $\hat{\mathcal{G}}^K$  depends on linear corrections to the self-energies  $\hat{\mathcal{L}}^R$  and  $\hat{\mathcal{L}}^K$ , which need to be computed self-consistently with  $\hat{\mathcal{G}}^K$ . This procedure is equivalent to take into account vertex corrections in the Kubo formalism. In our model, we assume isotropic scattering, in which case the vertex corrections vanish. This is a well known fact, and is ultimately due to the anti-symmetric form of the forces  $\mathbf{v}_F \cdot \mathbf{E}$  and  $\mathbf{v}_F \cdot \mathbf{r} \cdot \mathbf{T}$ . For cases of anisotropic impurity scattering (p-wave etc.), these corrections must be taken into account, as was done for the

diagonal response functions  $L_{11}$  and  $L_{22}$  by Durst and Lee.<sup>36</sup> In the following we neglect anisotropic scattering and compute all response functions  $L_{ij}$ .

The expression for  $\mathcal{G}^K$  given in the appendix of Ref. [18] is general enough to serve as the starting point

$$L_{12}^{ij} = \frac{e}{4} \int_{-Z}^Z d\epsilon \frac{\text{sech}^2 \frac{\epsilon}{2T}}{2T} \text{dp}_{\text{F}} [v_{\text{F},i} v_{\text{F},j}] \frac{N(\epsilon_{\text{F}}; \epsilon) - N_0^{\text{R}}(\epsilon)}{[N(\epsilon_{\text{F}}; \epsilon)]^2} = \frac{N_0^{\text{R}}(\epsilon)}{[N_0^{\text{R}}(\epsilon)]^2}; \quad (5)$$

where  $N(\epsilon_{\text{F}}; \epsilon) = N_{\text{F}} - N^{\text{R}}(\epsilon_{\text{F}}; \epsilon)$  is the density of states in the superconducting phase.  $L_{12}$  is directly proportional to the imaginary part of the unit term  $= N_0^{\text{R}}$  of the equilibrium impurity selfenergy, which is an odd function of energy. Eq. (5) is the proper generalization to arbitrary low temperatures, including impurity scattering renormalization effects, of the results in Refs. [23–24].

#### A. Conductivities

Once we know  $L^{ij}$ , we may compute the conductivities. In the following we consider transport in the cuprate planes, along one of the anti-nodes of the d-wave order parameter. We can then drop the superscripts of  $L^{ij}$ . The charge and heat conductances are given by

$$\begin{aligned} \kappa(T) &= \frac{L_{11}(T)}{T}; \\ \kappa(T) &= \frac{L_{22}(T)}{T^2}; \end{aligned} \quad (6)$$

In the presence of a temperature gradient, the non-vanishing thermoelectric coefficient  $L_{12}$  induces a charge current  $j_{\text{ch}} = -\kappa \nabla T$ , where we define

$$\kappa(T) = \frac{L_{12}(T)}{T^2}. \quad (7)$$

The appearance of a bulk charge current,  $j_{\text{ch}}$ , leads to a counter-flowing supercurrent, which we discuss in the next section.

In Fig. 2 we present the thermoelectric response function  $\kappa$  as a function of temperature for several phase shifts for a fixed rather short mean free path  $\ell = v_{\text{F}} \ell_0 / 50$ , where  $\ell_0 = v_{\text{F}} \tau_c$  is the superconducting coherence length. In our model, the physical transition temperature  $T_c$  is then suppressed by about 25% compared to the clean limit transition temperature  $T_{c0}$ , in accordance with the Abrikosov-Gorkov form for the  $T_c$ -suppression as function of  $\Gamma = (1/2) \Gamma_0$  by elastic impurity scattering.<sup>37</sup>  $\kappa(T)$  is sizable over a wide temperature range from zero to  $T_c$ , but vanishes in the  $T \rightarrow T_c$  limit, where the electron-hole asymmetry is of order  $s^2$  and neglected in our quasiclassical theory. The thermoelectric effect is sensitive to the microscopic superconducting

properties, such as the order parameter size and its symmetry, through the coherence factors entering Eq. (5). It is also sensitive to the nature of the impurity scattering: first to the normal state mean free path, but also to the phase shift  $\delta_0$ . In the strict Born ( $\delta_0 \rightarrow 0$ ) and unitary ( $\delta_0 \rightarrow \pi/2$ ) limits,  $\kappa(T)$  vanishes since the electron-hole asymmetry vanishes in those limits,  $= N_0^{\text{R}}(\epsilon) = 0$ . However, for all other values of  $\delta_0$ ,  $\kappa(T)$  is large, and has a maximum of the order of  $0.1 N_0^{\text{R}} = e$  near  $T = 0.5 T_c$ . Here  $N_0^{\text{R}} = e^2 N_{\text{F}} v_{\text{F}}^2 / (2)$  the Drude conductivity in the normal state. In fact, even a small deviation of the phase shift from e.g. the unitary limit leads to dramatic changes in the thermoelectric response, see below. At low temperature, we find  $\kappa \propto 1/T$ , (see left half of Fig. 2). The slope  $-\kappa/T$  contains detailed information about material parameters such as the scattering phase shift, as we will discuss in more detail in Section III.

We should mention that we have neglected inelastic scattering in our calculations. In e.g. Ref. [19] inelastic scattering by anti-ferromagnetic spin fluctuations were

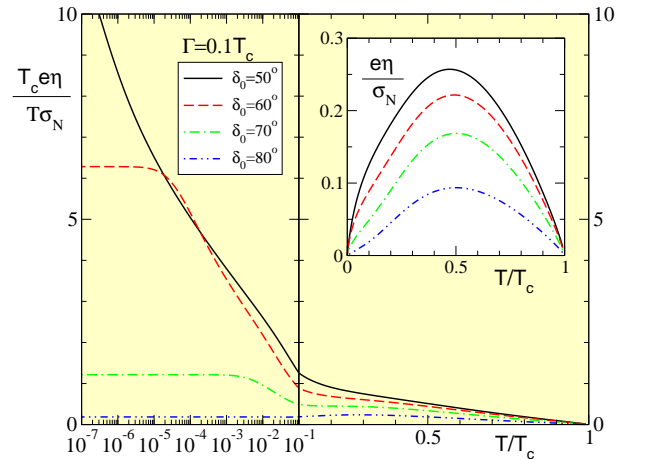


FIG. 2: The thermoelectric coefficient  $\kappa$  scaled by its low- $T$  dependence  $\kappa T$  for the scattering rate  $\Gamma = 0.1 T_c$  and several normal state scattering cross sections  $\sigma_i = \sin^2 \delta_0$ . The inset shows the unscaled function. In the universal limit  $\kappa(T)$ ,  $-\kappa/T$  approaches a non-universal constant given in Eq. (12).

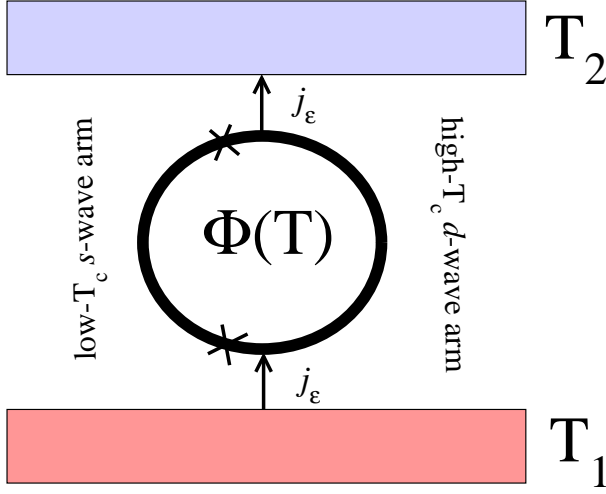


FIG. 3: A sketch showing the major features needed for the detection of thermoelectrically induced magnetic fluxes. The loop consists of two arms, one being an s-wave superconductor for which  $\lambda$  is orders of magnitude smaller than in the d-wave arm. The two superconductors are connected by Josephson junctions and the d-wave arm is connected to two bulky regions where the temperature is regulated.

included in the calculation of the thermal conductivity, and it was shown to give rise to the characteristic increase in  $\kappa(T)$  seen in experiments (e.g. [11,12]) just below  $T_c$ . Thus, we expect corrections to our results in Fig. 2 in the high temperature region  $T > T_c$ . In the important low- $T$  region,  $T < T_c$ , inelastic scattering is not of importance, since the corresponding self energy scales as  $T^3$  and is small compared to the self energy from elastic impurity scattering.

#### B. Thermoelectrically generated magnetic flux

In the normal state, the thermoelectric effect leads to the appearance of a voltage (given by the thermopower). However, in the superconducting state, a steady state voltage, and an associated electric field, is short circuited by the appearance of a supercurrent and an associated phase gradient,<sup>27,28,29</sup>

$$\mathbf{j}_s = (e\mathbf{m})n_s \mathbf{p}_s = \frac{1}{2} \nabla \Phi; \quad (8)$$

where  $n_s$  is the superfluid density and  $\mathbf{p}_s = \frac{1}{2} \nabla \Phi$  is the superfluid momentum. Thus, the total charge current is zero,  $\mathbf{j}_e^{\text{total}} = \mathbf{j}_d + \mathbf{j}_s = 0$ , but the phase gradient can be detected in a flux measurement as was done in Ref. [30,31]. These early experiments were carried out with low- $T_c$  s-wave superconductors, for which thermoelectric effects are smaller than in the unconventional superconductors we are considering, for two reasons. First, they are down by the electron-hole asymmetry factor  $s$ ; second, they are exponentially suppressed at low temperatures by the energy gap around the Fermi surface.

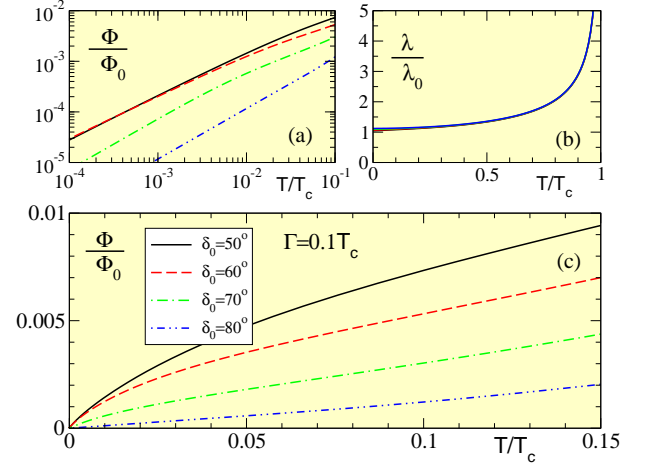


FIG. 4: The magnetic flux induced by a temperature gradient in a ring with a thermoelectric response given in Fig. 2. It is assumed that a temperature difference  $\Delta T = T_1 - T_2 = 0.005T_c$  is maintained over the loop in Fig. 3. Current experimental precision for flux measurements is  $10^{-6} \Phi_0 = \text{Hz}$ . Part (b) shows the divergence of the penetration depth in the d-wave superconductor at temperatures near  $T_c$ .

Consequently, the experiments were mainly done in the temperature region near  $T_c$ , where the temperature dependence of  $n_s$  plays an important and somewhat parasitic role when the goal is to measure  $\kappa(T)$  (for a recent discussion of the experimental situation see Ref. [38]).

To measure the flux generated by the counter-flowing supercurrent, we propose a hybrid SQUID-like setup, as indicated in Fig. 3, with one arm of a low- $T_c$  material and the other of the cuprate material of interest. The two arms are in electrical contact via two Josephson junctions. Thus, by construction, the generated flux will mainly originate from the cuprate arm and we can predict a non-quantized flux of size

$$\frac{\Phi(T)}{\Phi_0} = n_2 + \frac{\Phi(T)^2}{2} \frac{e(T)}{N} \frac{T}{N} + O(s^2); \quad (9)$$

Here  $\Phi_0 = c_0/2e$  is the flux quantum,  $c_0$  the velocity of light,  $T = T_1 - T_2$  the temperature bias,  $\Phi_0 = \frac{c_0^2}{4e^2 N_F v_F^2}$  the zero-temperature penetration depth in the clean system, and  $\Phi(T) = \frac{p}{c_0^2 m} = \frac{p}{4e^2 n_s}$  the temperature dependent penetration depth in the dirty system. We assume that the equilibrium flux is zero and put the integer  $n = 0$  hereafter. The superfluid momentum is proportional to the local temperature gradient  $\nabla T$ , which leads to that the flux is proportional to the temperature bias  $T$ , since  $\Phi$  is related to a contour integral of  $\mathbf{p}_s$  around the loop (the evaluation of  $\Phi$  is a standard calculation that can be found in e.g. Ref. [31]). Note that if both arms were of the same material, the thermoelectric response in the two arms would give counter-flow in opposite directions around the loop and cancel. It is therefore necessary to have different responses in the two arms, although it does not matter

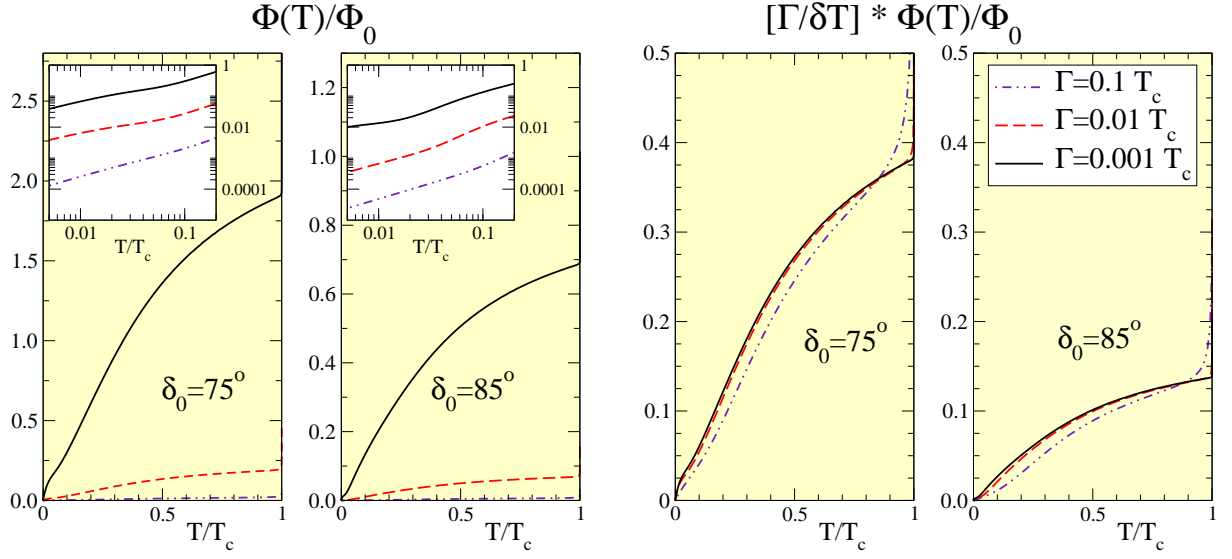


FIG. 5: The thermoelectrically induced flux as a function of temperature for strong scattering in purity potentials,  $\delta_0 = 75^\circ$  (left) and  $\delta_0 = 85^\circ$  (right), at different scattering rates (the corresponding mean-free-paths are: 5, 50, and 500  $\xi_0$ ). In the two left panels we show the actual flux generated as a function of temperature, setting  $T = 0.005T_c$ . At high temperatures,  $T \sim T_c$ , the flux is a sizable fraction of  $\Phi_0$  and a larger  $T$  may well give a flux  $\sim \Phi_0$ . At low temperatures  $T \ll 0.1T_c$  the flux may still be of order 0.1%–1%  $\Phi_0$  if the material is clean,  $\ell \sim 20\xi_0$ , as indicated in the insets. In the two panels to the right we show the factor  $(\Gamma(T) = \Phi_0)^2 e^{-\Gamma(T) = N}$ . This factor depends strongly on the scattering phase shift  $\delta_0$  (see also Fig. 2 where  $e^{-\Gamma(T) = N}$  is displayed for a larger variety of scattering phase shifts) but does not have a particularly strong dependence on  $\delta_0$  apart from close to  $T_c$  where the temperature dependence of  $\Gamma(T)$  dominates.

how that is achieved. Our setup is limited to low temperatures by the low transition temperature  $T_c \sim 15$  K of the s-wave superconductor. To probe the high temperature regime of Eq. (9), some other type of asymmetry in the thermoelectric response of the two arms must be accomplished. Disregarding these complications, we now investigate Eq. (9) for all temperatures below  $T_c$  of the d-wave arm.

In Fig. 4 we give an estimate of the induced flux corresponding to the thermoelectric response in Fig. 2, assuming a temperature difference of  $0.005T_c \sim 0.5$  K maintained across the loop. When the scattering phase shift is intermediate between the Born and unitary limits, fluxes of order of 0.1%–1% of the flux quantum is generated at  $^4\text{He}$  temperatures  $4.2$  K ( $\sim 0.05T_c$ ). At higher temperatures the temperature difference could be allowed to be larger and we can predict fluxes on the order of 10% of  $\Phi_0$ . For cleaner samples, the induced flux can be even larger, of the order of a few percent of  $\Phi_0$  at  $T = 0.05T_c$ , see Fig. 5.

For high temperatures, the temperature dependence of the flux is heavily influenced by the temperature dependence of the penetration depth, see Fig. 4 and Fig. 5. Thus, to extract the  $T$ -dependence of  $\Gamma(T)$  from  $\Gamma(T)$ , the temperature dependence of  $\Gamma(T)$  should be divided out. However, in the important low-temperature regime (to be discussed further in the following section),  $\Gamma$  is directly proportional to  $\Gamma(T)/T$ , since the penetration depth is limited by impurity scattering,<sup>37,39</sup>  $\Gamma(T) \sim \Gamma(0)/T^2$ , and its  $T$ -dependence can be neglected.

We note that the minimum temperature at which measurements can be performed will be set by a combination of two factors: first, the smallest temperature bias that can be applied ( $T - T_c$ ) is needed in order to have a uniform thermoelectric response function  $\Gamma(T)$  in the sample; second, the flux measurement sensitivity, since the flux scales as  $\Gamma(T) T - T_c$ . Thus, at low temperatures, there is a trade-off between having a small  $T - T_c$  and at the same time have a measurable flux.

Note that the induced superfluid momentum  $p_s$  is small. We estimate

$$\frac{v_F p_s}{T_c} \sim \frac{\Phi_0}{L} \frac{1}{\Phi_0}; \quad (10)$$

where  $L$  is the distance between the two reservoirs (i.e. we have set  $r = T = T_c$ ). Thus, we do not need to take feedback effects from the superflow via the Doppler shifts into account.

### III. LOW TEMPERATURES

In the low- $T$  limit, the response functions  $L$  can be studied analytically through a systematic Sommerfeld expansion in the small parameter  $T = T_c$ . The magnitude of  $L$  depends on the normal state scattering rate as well as the phase shift, and we have  $\Gamma_0 = 2$  in the unitary limit while  $\Gamma_0 \exp[\Gamma_0 = 2]$  in the Born limit. For intermediate phase shifts ( $\delta_0$ ) can be found numerically as we discuss below. Only in the limit  $T$



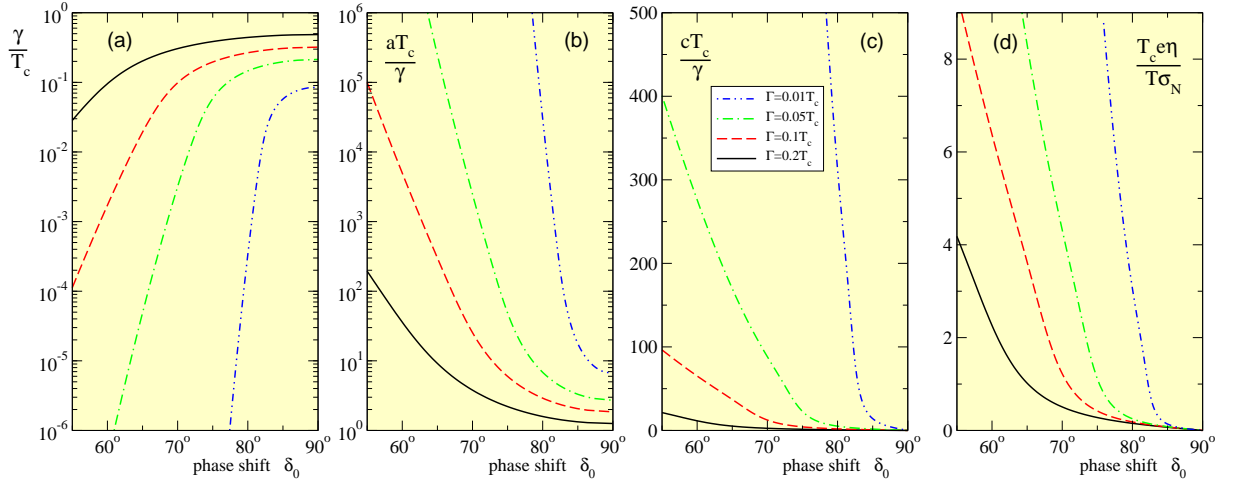


FIG. 6: (a)–(c) Phase-shift dependence of the impurity band width  $\gamma$  and the parameters  $a$  and  $c$  normalized by  $\gamma = T_c$ , see Eqs. (A 1)–(A 3). (d) The thermoelectric coefficient  $\eta = T$  at low temperatures  $T \ll T_c$ . The dashed (red) curve contains the low- $T$  constants in Fig. 2. We have used  $\langle p_x \rangle = v_0 \cos 2\phi_f$  throughout.

is the Sommerfeld expansion useful. Thus, we consider low energies and write

$$\begin{aligned} \tilde{\epsilon}^R &= a + i(b^2) + d^3 + O[\epsilon^4]; \\ \tilde{\epsilon}^I &= c + h^3 + O[\epsilon^5]; \end{aligned} \quad (11)$$

with real constants  $a, b, c, d, h$ , and  $\epsilon$ . These constants are determined self-consistently by the low-energy equations presented in the appendix. Inserting this ansatz into Eq. (5), keeping terms to leading order in  $\epsilon$ , we find for the thermoelectric response

$$\frac{\langle T \rangle}{T} = e^2 \frac{2N_f v_f^2}{3} \frac{c}{v_0} \left( 1 + \frac{7}{15} \frac{a_{12}^2 T^2}{v_0^2} \right); \quad (12)$$

where  $\epsilon = (1 - v_0) \hbar v_f / d$  is the opening rate of the gap at the nodes (related to the so called gap velocity, see Ref. [36]). The coefficient of the  $T^2$  correction to the  $T \rightarrow 0$  asymptotic is given by

$$a_{12}^2 = a^2 + 2c^2 + \frac{3h^2}{c} \quad (13)$$

Including phase shifts away from the unitary and the Born limits will also change the rate at which the charge and heat conductivities approach their universal values. We find the leading order dependence of the charge conductivity to be

$$\frac{\langle T \rangle}{T} \approx e^2 \frac{2N_f v_f^2}{3} \frac{c}{v_0} \left( 1 + \frac{2}{3} \frac{a_{11}^2 T^2}{v_0^2} \right); \quad (14)$$

and of the heat conductivity to be

$$\frac{\langle T \rangle}{T} \approx \frac{2}{3} \frac{2N_f v_f^2}{v_0} \left( 1 + \frac{7}{15} \frac{a_{22}^2 T^2}{v_0^2} \right); \quad (15)$$

where the coefficients of the  $T^2$ -terms contain direct information about the impurity induced particle-hole

asymmetry through the parameters  $a$  and  $c$ ,

$$\begin{aligned} a_{11}^2 &= a^2 + c^2; \\ a_{22}^2 &= a^2 + 2c^2; \end{aligned} \quad (16)$$

In the zero temperature limit  $T \rightarrow 0$ , both the charge and heat conductivities approach universal values (independent of the properties of the impurities) while  $\eta = T$  has a non-universal  $T \rightarrow 0$  limit set by the ratio  $c = \gamma$ . All functions, including  $\eta$ , have non-universal low- $T$  corrections to their  $T = 0$  values and are sensitive to the phase shift  $\phi_0$  and the scattering rate  $\Gamma$ . We note that the low- $T$  expressions given in Ref. [18] for  $\eta$  and  $\eta = T$  were implicitly restricted to the unitary and Born limits. Consequently, the parameter  $c$  is absent in their Eqs. (56)–(57).

We can analyze these results further by solving the self-consistency equations for the impurity self-energy to lowest order in  $\epsilon$ , and thereby determine the parameters  $\gamma, a, c$ , etc. The results are given in the appendix, Eqs. (A 1)–(A 6), and the numerical solution is presented in Figs. 6–7. The impurity band width  $\gamma$  is exponentially small for phase shifts far from the unitary limit. As a consequence, the universal limit is reached at an exponentially small temperature. This is also confirmed in the left half of Fig. 2, where we present the thermoelectric response function on a logarithmic scale. Clearly, the crossover to the low- $T$  power law is severely pushed down in  $T$  for small phase shifts. This suppression becomes extremely fast when the system is clean. In fact, for ultra-clean samples, with  $\Gamma \leq 10^{-3} T_c$  or lower (corresponding to normal state mean free paths  $\ell \geq 500 \ell_0$  or longer), a deviation of the phase shift away from  $\phi = \pi/2$  by only a few percent will reduce  $\gamma$  by several orders of magnitude, see Fig. 7(a). At the same time, the ratio  $c = \gamma$  is increased humongously [Fig. 6(c)],  $\eta = T$  grows large [Fig. 7(c)] and the thermoelectric coefficient itself is sizable on the scale of  $\eta_N = e$  [Fig. 7(d)].

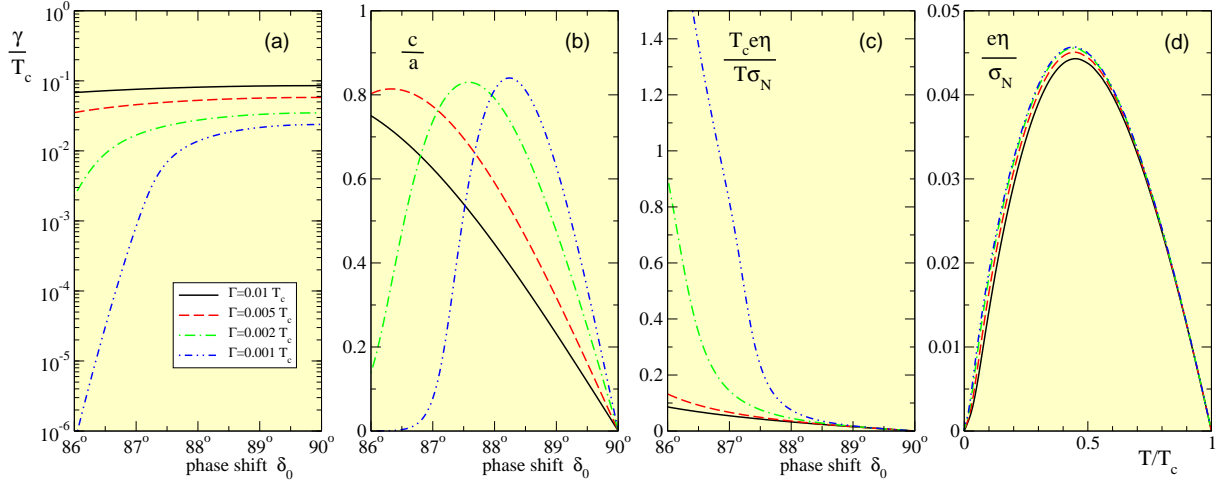


FIG. 7: (a) The impurity band width is extremely sensitive to phase shift variations in clean systems. (b) The ratio of the parameters  $c$  and  $a$ . (c) The low- $T$  asymptotic of the thermoelectric coefficient grows large even for small deviations of the phase shift from the unitary limit. (d) The temperature dependence of the thermoelectric response function for a phase shift  $\delta_0 = 86.4^\circ$  ( $\sin^2 \delta_0 = 0.996$ ). Note the data collapse when  $\eta$  is scaled by  $\sigma_N = e$ , because  $\gamma$  grows as  $1/\sigma_N$  in clean systems.

The thermoelectric response scales as  $1/\sigma_N$ , which is also clear in Fig. 5. Thus, if we change the normalization in Fig. 7 (c)–(d) from the normal state Drude conductivity  $\sigma_N$  (which effectively cancels this scaling), to the universal limit charge conductance  $(T = 0) = \sigma_0$  in Eq. (14), we get the scale  $T_c e \eta = (T = 0) = 100 - 1000$  in Fig. 7 (c), and  $e \eta = 0.01 - 0.001 T_c$  in Fig. 7 (d), for  $0.01 - 0.001 T_c$ . Thus, the thermoelectric effect grows large in clean systems with phase shifts close to the unitary limit.

Note the equal importance of the parameters  $c$  and  $a$  in a region near the unitary limit, see Figs. 6 (b)–(c) and Fig. 7 (b). The ratio approximately behaves as  $c/a = (\sin \delta_0 / \cos \delta_0)$ . Thus, unless  $\delta_0 \approx \pi/2$  (which holds far from the unitary limit deep inside the region where  $\gamma$  is exponentially suppressed) it is in general not allowed to neglect the unit term when conductivities are computed at intermediate phase shifts, although that has been common in the literature (e.g. in [15,20,36]).

Finally, by comparing Figs. 6 and 2 we see that the true universal limit is in fact reached at very small temperatures,  $T \ll 10^{-2}$ . This is due to the largeness of the parameters  $a$  and  $c$  [c.f. Fig. 6 (b)–(c)] and higher order parameters  $b$ ,  $d$ , and  $h$ , for clean systems with phase shifts near but not strictly equal to  $\pi/2$ . Thus, we need  $T \ll (a) = (c)$  in order for the Sommerfeld expansion to work well. Or, strictly speaking, we have an effective Sommerfeld expansion parameter  $T = (a)$ , instead of  $T = (c)$ .

#### IV. SUMMARY AND CONCLUSIONS

In this paper we have focused on phase shifts close to  $\pi/2$ , because that appears to be the relevant region experimentally. Perhaps the most clear signature of this is the impurity induced resonances seen in STM

experiments.<sup>21</sup> The resonance energy is near the Fermi level, but not at the Fermi level, thus signaling a phase shift close to  $\pi/2$ . Also, if the low temperature heat conductivities found in experiments<sup>2,4,6,8,10,11,12</sup> are indeed universal, the phase shift needs to be close to  $\pi/2$ . Otherwise,  $\gamma$  is exponentially suppressed and it would be hard to argue that the limit  $T \rightarrow 0$  was reached. The limit  $\delta_0 = \arctan(N_F u_0) \approx \pi/2$  can in real life of course only be approached asymptotically. It is therefore likely that thermoelectric effects are of importance in the high- $T_c$ , as well as other unconventional superconductors (universal heat conductance was also found in  $\text{Sr}_2\text{RuO}_4$  [9]). The effect grows large in clean systems. The ideal experiment would then be to measure the thermoelectrically induced flux, together with the thermal conductivity, at low temperatures for samples with different levels of disorder, e.g. through controlled Zn doping. The slope of the thermal conductivity is related to the gap size  $\delta_0$  and its slope at the node, through  $(\delta_0^2 = 3)(2N_F v_F^2) = (\delta_0)$ , which can be compared with values of  $\delta_0$  and from other experimental probes (e.g. photoemission<sup>40</sup>). The ratio  $(e) = (c)$  contains information about  $\delta_0$  through Eqs. (A1)–(A3), with  $\delta_0$  and  $\gamma$  as input parameters. We note that the exact angle dependence of the gap function is not particularly important and it is enough to know  $\delta_0$  and  $\gamma$ . If the normal state scattering rate is known independently, the scattering phase shift is uniquely determined by  $\gamma = (e)$ .

When the energy scale  $\gamma$  is exponentially suppressed in clean systems, the temperature region in which the  $T^2$  term in the expansions in Eq. (12)–(15) is of importance, is also suppressed. Thus, it is not necessarily ideal to study super-clean samples. Another issue with super-clean samples is the validity of the homogeneous scattering model with only s-wave scattering, in which a dilute concentration of point impurities are assumed to be ran-

domly distributed in the sample. For sufficiently clean samples this model has to be broken down and should be replaced by more realistic models of extended impurities (suggestions can be found in e.g. Refs. [41,42,43]).

In conclusion, we have computed the thermoelectric effect in unconventional superconductors with impurities scattering in neither the Born nor the unitary limits. The thermoelectric effect is an interesting unexplored avenue for the investigation of microscopic properties of high- $T_c$  as well as other unconventional superconductors, in particular at low temperatures. Of special interest is to extract material parameters such as the gap size  $\Delta_0$ , the slope of the gap at the gap node  $\Delta' = (1/\Delta_0) d\Delta/dj_{\text{node}}$ , the impurity band width  $\Gamma$ , and the impurity scattering rate and phase shift  $\phi_0$ . This can be accomplished by measuring the universal values of the transport coefficients and at  $T \rightarrow 0$ , and possibly their low- $T$  corrections. We add to this arsenal of tools the thermoelectric coefficient, which at low temperatures scales linearly with temperature, with a non-universal slope.

#### Acknowledgments

We gratefully acknowledge valuable discussions with V. Chandrasekhar, P. Delsing, M. Eschrig, Yu. Galperin, Z. Jiang, J. A. Sauls, V. S. Shumeiko, A. Vorontsov, and A. Yurgens. Financial support was provided by STINT, the Swedish Foundation for International Cooperation in Research and Higher Education (T.L.), the Wenner-Gren Foundations (T.L.), and the Swedish Research Council (M.F.).

#### APPENDIX A: IMPURITY SELF-ENERGY AT LOW ENERGIES

The ansatz in Eq. (11) can be used together with the expression for the self energy in Eq. (4) to self-consistently compute the parameters  $a, b, c, d, h$ , and  $\dots$ . Actually, only  $a$  need to be computed self-consistently; the other parameters immediately follow. To lowest or-

der,  $\phi_0$ , we obtain

$$a = \frac{J_1}{1 - i + i J_1^2}; \quad (\text{A } 1)$$

where  $J_1$  is the first of a series of Fermi surface integrals

$$J_n = J_n(\phi_0) = \int_{-\pi}^{\pi} d\phi_f \frac{1}{2(p_f)^2 + 2^{n-2}}; \quad (\text{A } 2)$$

where  $n$  is an integer (only odd  $n$  appears here). In the next order,  $\phi_1$ , we get

$$a = \frac{J_1 D^{-1}}{1 - i + i J_1^2}; \quad (\text{A } 3)$$

where  $D = 2 - i J_1 (J_1 - J_3) + J_3$ . The next order,  $\phi_2$ , is more complicated, but can be expressed in terms of the following functions

$$\begin{aligned} k_0 &= J_1; \\ k_1 &= \frac{a}{2} (J_1 - J_3); \\ k_2 &= \frac{b}{2} (J_1 - J_3) + \frac{3a^2}{2^2} (J_3 - J_5); \\ k_3 &= \frac{d}{2} (J_1 - J_3) + \frac{1a^3}{2^3} - \frac{3ab}{2} (J_3 - J_5) \\ &\quad - \frac{5a^3}{2^3} (J_5 - J_7); \end{aligned} \quad (\text{A } 4)$$

and

$$\begin{aligned} m_0 &= 1 - i + i k_0^2; \\ m_1 &= \frac{2}{m_0} i k_0 k_1; \\ m_2 &= \frac{i}{m_0} (k_1^2 - 2k_0 k_2); \\ m_3 &= \frac{2}{m_0} i (k_0 k_3 + k_1 k_2); \end{aligned} \quad (\text{A } 5)$$

We get

$$\begin{aligned} b &= D^{-1} - 2i J_1 (J_1 - J_3) a (a - 1) + \frac{a^2}{2} \frac{3}{2} (J_3 - J_5) (2 - i J_1) + i (J_1 - J_3)^2; \\ d &= D^{-1} - (2 - i J_1) \frac{1a^3}{2^3} - \frac{3ab}{2} (J_3 - J_5) - \frac{5a^3}{2^3} (J_5 - J_7) + m_0 m_1 b + m_0 m_2 (1 - a) - 2i k_1 k_2; \\ h &= \frac{1}{1 - i + i m_0^2} m_1^3 + 2m_1 m_2 - m_3; \end{aligned} \quad (\text{A } 6)$$

The Fermi surface integrals can in general be computed through recursion ( $n = 1, 3, 5, \dots$ ),

$$J_{n+2} = J_n - \frac{dJ_n}{n d\phi_0}; \quad (\text{A } 7)$$

To get explicit expressions we need a model of the order parameter. For the numerics in this paper we



use for simplicity  $(\epsilon_f) = \epsilon_0 \cos(2\theta_f)$ , in which case  $J_1 = (2\pi)^{-1} \int_0^{2\pi} K[k] dk$ , where  $k = 1/\sqrt{1 + (\epsilon_0)^2}$  and  $K[k]$  is the complete elliptic integral of the first

kind.<sup>44</sup> In this case  $J_3 = (2\pi)^{-1} \int_0^{2\pi} E[k] dk$ , where  $E[k]$  is the complete elliptic integral of the second kind, and the other  $J_n$  follow by recursion.

- 
- Electronic address: tom.as@snowmass.phys.nyu.edu
- <sup>y</sup> Electronic address: mikael.fogelstrom@c2.chalmers.se
- <sup>1</sup> D. A. Bonn, P. D. Osanj, R. Liang, and W. N. Hardy, Phys. Rev. Lett. 68, 2390 (1992).
- <sup>2</sup> L. Taillefer, B. Lussier, R. Gagnon, K. Behnia, and H. Aubin, Phys. Rev. Lett. 79, 483 (1997).
- <sup>3</sup> A. Hosseini, R. Harris, S. Kamal, P. D. Osanj, J. Preston, R. Liang, W. N. Hardy, and D. A. Bonn, Phys. Rev. B 60, 1349 (1999).
- <sup>4</sup> M. Chiao, R. W. Hill, C. Lupien, L. Taillefer, P. Lambert, R. Gagnon, and P. Fournier, Phys. Rev. B 62, 3554 (2000).
- <sup>5</sup> J. Corson, J. Orenstein, S. Oh, J. O'Donnell, and J. N. Eckstein, Phys. Rev. Lett. 85, 2569 (2000).
- <sup>6</sup> S. Nakamae, K. Behnia, L. Balicas, F. Rullier-Abenque, H. Berger, and T. Tamegai, Phys. Rev. B 63, 184509 (2001).
- <sup>7</sup> R. W. Hill, C. Proust, L. Taillefer, P. Fournier, and R. L. Greene, Nature 414, 711 (2001).
- <sup>8</sup> Y. Ando, J. Takeya, Y. Abe, S. F. Sun, and A. N. Lavrov, Phys. Rev. Lett. 88, 147004 (2002).
- <sup>9</sup> M. Suzuki, M. A. Tanatar, N. Kikugawa, Z. Q. Mao, Y. Maeno, and T. Ishiguro, Phys. Rev. Lett. 88, 227004 (2002).
- <sup>10</sup> C. Proust, E. Boaknin, R. W. Hill, L. Taillefer, and A. P. Mackenzie, Phys. Rev. Lett. 89, 147003 (2002).
- <sup>11</sup> M. Sutherland, D. G. Hawthorn, R. W. Hill, F. Ronning, S. Wakimoto, H. Zhang, C. Proust, E. Boaknin, C. Lupien, L. Taillefer, et al., Phys. Rev. B 67, 174520 (2003).
- <sup>12</sup> R. W. Hill, C. Lupien, M. Sutherland, E. Boaknin, D. G. Hawthorn, C. Proust, F. Ronning, L. Taillefer, R. Liang, D. A. Bonn, et al., Phys. Rev. Lett. 92, 027001 (2004).
- <sup>13</sup> P. J. Tumer, R. Harris, S. Kamal, M. E. Hayden, D. M. Broun, D. C. Morgan, A. Hosseini, P. D. Osanj, G. K. Mullins, J. S. Preston, et al., Phys. Rev. Lett. 90, 237005 (2003).
- <sup>14</sup> C. J. Pethick and D. Pines, Phys. Rev. Lett. 57, 118 (1986).
- <sup>15</sup> P. J. Hirschfeld, P. Wole, and D. Einzel, Phys. Rev. B 37, 83 (1988).
- <sup>16</sup> P. A. Lee, Phys. Rev. Lett. 71, 1887 (1993).
- <sup>17</sup> P. J. Hirschfeld, W. O. Putikka, and D. J. Scalapino, Phys. Rev. Lett. 71, 3705 (1993).
- <sup>18</sup> M. J. Graft, S.-K. Yip, J. A. Sauls, and D. Rainer, Phys. Rev. B 53, 15147 (1996).
- <sup>19</sup> P. J. Hirschfeld and W. O. Putikka, Phys. Rev. Lett. 77, 3909 (1996).
- <sup>20</sup> W. K. In, F. Marsiglio, and J. P. Carbotte, Phys. Rev. B 68, 174513 (2003).
- <sup>21</sup> S. H. Pan, E. W. Hudson, K. M. Lang, H. Eisaki, S. Uchida, and J. C. Davis, Nature 403, 749 (2000).
- <sup>22</sup> H. Monien, K. Schamberg, and D. Walker, Solid State Commun. 63, 263 (1987).
- <sup>23</sup> B. Ar, H. Bahlouli, C. J. Pethick, and D. Pines, Phys. Rev. Lett. 60, 2206 (1988).
- <sup>24</sup> B. Ar, H. Bahlouli, and C. J. Pethick, Phys. Rev. B 39, 8959 (1989).
- <sup>25</sup> M. I. Salkola, A. V. Balatsky, and D. J. Scalapino, Phys. Rev. Lett. 77, 1841 (1996).
- <sup>26</sup> P. J. Hirschfeld, Phys. Rev. B 37, 9331 (1988), in this work the thermoelectric effect in heavy fermion systems was also considered. But the source of electron-hole asymmetry was small, of higher order in quasiclassical expansion parameters, compared to the one considered in Ref. [23,24] and by us, although it was argued that the response could be enhanced by the large effective mass.
- <sup>27</sup> V. L. Ginzberg, Zh. Eksp. Teor. Fiz 14, 177 (1944).
- <sup>28</sup> Y. M. Gal'perin, V. L. Gurevich, and V. I. Kozub, Zh. Eksp. Teor. Fiz 66, 1387 (1974).
- <sup>29</sup> J. C. Garland and D. J. van Harlingen, Phys. Lett. A 47, 423 (1974).
- <sup>30</sup> N. V. Zavaritskii, Pis'ma Zh. Eksp. Teor. Fiz 19, 126 (1974).
- <sup>31</sup> D. J. van Harlingen, D. F. Heidel, and J. C. Garland, Phys. Rev. B 21, 1842 (1980).
- <sup>32</sup> G. D. Mahan, Many-Particle Physics, 2nd ed. (Plenum Press, New York, 1990).
- <sup>33</sup> A. V. Balatsky, M. I. Salkola, and A. Rosengren, Phys. Rev. B 51, 15547 (1995).
- <sup>34</sup> A. A. Abrikosov, L. P. Gor'kov, and I. E. Dzyaloshinski, Methods of Quantum Field Theory in Statistical Physics (Dover Publications, Inc., New York, 1975).
- <sup>35</sup> D. Rainer and J. A. Sauls, in Superconductivity: From Basic Principles to the Latest Developments, edited by L. N. Butcher and Y. Lu (World Scientific, Singapore, 1995), pp. 45-78.
- <sup>36</sup> A. C. Durst and P. A. Lee, Phys. Rev. B 62, 1270 (2000).
- <sup>37</sup> D. Xu, S.-K. Yip, and J. A. Sauls, Phys. Rev. B 51, 16233 (1995).
- <sup>38</sup> Y. M. Gal'perin, V. L. Gurevich, V. I. Kozub, and A. L. Shelankov, Phys. Rev. B 65, 064531 (2002).
- <sup>39</sup> P. J. Hirschfeld and N. Goldenfeld, Phys. Rev. B 48, 4219 (1993).
- <sup>40</sup> A. Damascelli, Z. Hussain, and Z.-X. Shen, Rev. Mod. Phys. 75, 473 (2003).
- <sup>41</sup> I. Adagideli, D. E. Sheehy, and P. M. Goldbart, Phys. Rev. B 66, 140512 (2002).
- <sup>42</sup> D. E. Sheehy, Phys. Rev. B 68, 054529 (2003).
- <sup>43</sup> Y. G. Pogorelov and M. C. Santos, cond-mat/0402199.
- <sup>44</sup> I. S. Gradshteyn and I. M. Ryzhik, Tables of Integrals, Series, and Products, Fifth Edition (Academic Press, San Diego, 1994).